Acta Crystallographica Section F
Structural Biology Communications
ISSN 2053-230X

Characterization, crystallization and preliminary X-ray crystallographic analysis of the human Uba5 C-terminus–Ufc1 complex

Shutao Xie

MOE Key Laboratory of Protein Science, School of Life Sciences, Tsinghua University, Beijing 100084, People's Republic of China

Correspondence e-mail: xieshutao@sina.com

Received 13 May 2014
Accepted 19 June 2014

Human Uba5, which contains an adenylation domain and a C-terminal region, is the smallest ubiquitin-like molecule-activating enzyme. The mechanism through which the enzyme recognizes Ufc1 and catalyzes the formation of the Ufc1–Ufm1 complex remains unknown. In this study, Uba5 residues 364–404 were demonstrated to be necessary for the transthiolation of Ufm1 to Ufc1, and Uba5 381–404 was identified to be the minimal region for Ufc1 recognition. The fusion protein between Uba5 381–404 and Ufc1 was cloned, expressed and purified, and exists as a homodimer in solution. Crystallization was performed at 293 K using PEG 4000 as precipitant; the optimized crystals diffracted to 3.0 Å resolution and had unit-cell parameters $a = b = 82.49$, $c = 62.47$ Å, $\alpha = \beta = 90$, $\gamma = 120^\circ$. With one fusion-protein molecule in the asymmetric unit, the Matthews coefficient and solvent content were calculated to be 2.55 Å^3 Da^{-1} and 51.84%, respectively.

1. Introduction

Protein modification by covalent attachment of ubiquitin and ubiquitin-like molecules (UBLs) plays an essential role in the function and regulation of many molecular processes in all eukaryotic organisms (Goldberg, 2007; Schulman & Harper, 2009). Three kinds of enzymes are involved in this activation cascade, including UBL activating enzyme (E1), UBL conjugation enzyme (E2) and UBL ligase (E3). Different UBLs have distinct E1s. Based on domain architecture, these E1s are divided into canonical and noncanonical E1s (Schulman & Harper, 2009). Canonical E1s contain an inactive adenylation domain, an active adenylation domain, the first conserved catalytic cysteine domain (FCCH), the second conserved catalytic cysteine domain (SCCH) and a C-terminal ubiquitin-fold domain. Noncanonical E1s comprise Uba4, Uba5 and Atg7, and they differ greatly from canonical E1s in molecular weight, domain architecture and the mechanisms underlying the activation of their corresponding UBLs.

Ubiquitin-fold modifier 1 (Ufm1) belongs to the UBL family with a dedicated E1 (Uba5), E2 (Ufc1) and E3 (Ufl1) (Komatsu *et al.*, 2004; Dou *et al.*, 2005; Tatsumi *et al.*, 2010). The Uba5–Ufm1 modification system is conserved in metazoans and plants, but not in yeasts, suggesting an important role in multicellular organisms (Komatsu *et al.*, 2004; Gannavaram *et al.*, 2011; Zhang *et al.*, 2012; Hertel *et al.*, 2013). Previous studies have shown that Uba5 is important for cell autonomous erythroid differentiation and is involved in the regulation of haematopoiesis (Tatsumi *et al.*, 2011). Uba5 comprises only an adenylation domain (AD) followed by a C-terminal domain (CTD), with the canonical FCCH and SCCH domains being absent (Fig. 1*a*). The N-terminal residues (1–56) of Uba5 are not conserved among different species, and are unnecessary for Ufm1 activation (Zheng *et al.*, 2008). The crystal structure of the Uba5 adenylation domain (residues 57–329; PDB entry 3h8v, Bacik *et al.*, 2010) reveals that the adenylation domain is similar to that of its E1 homologues. Ufc1 is the downstream E2 for Uba5. Although Ufc1 shares low sequence

identity with the canonical E2, their structures are topologically similar (Mizushima *et al.*, 2007; Liu *et al.*, 2009). Despite these advances, the mechanism underlying Ufc1 recognition by Uba5 and the subsequent formation of the Ufc1–Ufm1 complex remains ambiguous.

This study shows that the Uba5 C-terminal domain is necessary for the transthiolation of Ufm1 to Ufc1. The minimal region of Uba5 required for Ufc1 recognition was identified. The expression, purification, crystallization and preliminary X-ray crystallographic analysis of the fusion protein between Uba5 381–404 and Ufc1 are also reported. These results provide a basis for further understanding the molecular mechanisms of Uba5-mediated Ufc1 recognition and Ufm1 transthiolation.

2. Materials and methods

2.1. Cloning

Five constructs of *Homo sapiens* Uba5 (EC 6.3.2.19, NCBI accession No. NM_024818.3) were prepared in this study (Fig. 1*a*). Uba5 57–363, 57–404 and Ufc1 (EC 6.3.2.19, NCBI accession No. NP_057490.2) were amplified by PCR from cDNA plasmids, digested with the restriction endonucleases *Nde*I and *Xho*I (New England Biolabs) and ligated into the vector pETDuet-1 (Novagen). The GST-tagged Uba5 C-terminal fragments (330–404, 364–404 and 381–404) were amplified, digested with *Nde*I and *Xho*I, and ligated into the vector pGEX-6P-1 (GE Healthcare). Empty pGEX-6P-1 vector was used for the expression of GST proteins. The Uba5 381–404~Ufc1 fusion protein was amplified using two-round PCR. In the first round, two primers (5′-CATGGCCAAAATGAAGAATATGGGCTCTGGCTCTGGCTCTGGCTCTATGGCGGATGAAGCCACGCGA-3′ and 5′-TCGCGTGGCTTCATCCGCCATAGAGCCAGAGCCAGAGCCAGAGCCCATATTCTTCATTTTGGCCATG-3′) were used to generate a fused Uba5-Ufc1 template linked by a four Gly-Ser repeat coding sequence. The fusion protein was then amplified by PCR using primers containing *Nde*I and *Xho*I sites. The second-round PCR products were digested and ligated into the vector pETDuet-1. The ligated products were then transformed into *Escherichia coli* DH5α competent cells and the positive transformants were selected from agar plates containing 100 µg ml^{-1} ampicillin. The authenticity of the construct was confirmed by DNA sequencing.

2.2. Expression and purification

The recombinant plasmids for Uba5 57–363, Uba5 57–404, Ufc1, Uba5 381–404~Ufc1, Uba5 330–404, 364–404, 381–404 and empty

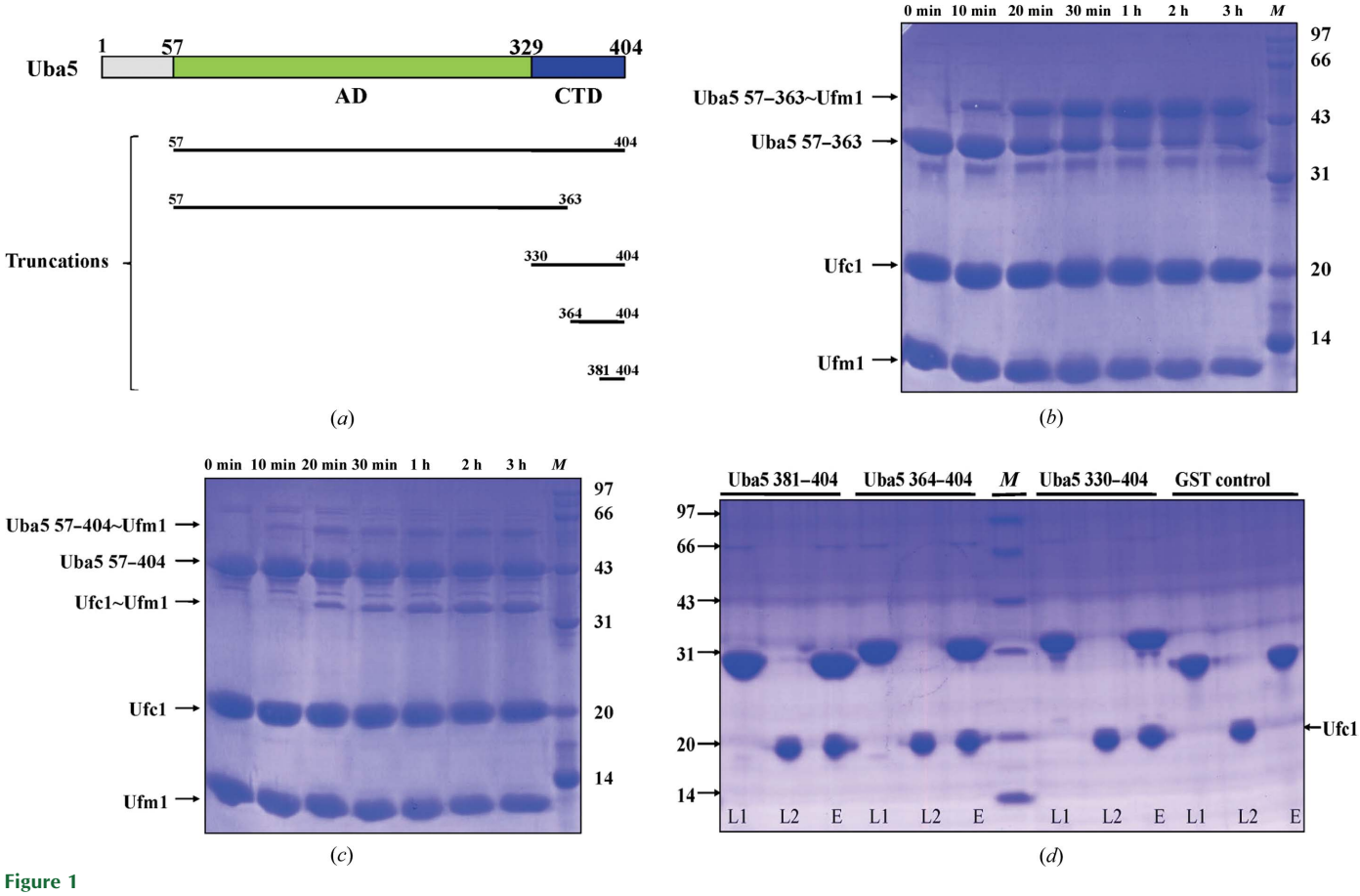

Figure 1
Uba5 domain architecture and *in vitro* assays. (*a*) Overview of Uba5 and the five Uba5 constructs used in this study. Uba5 comprises an adenylation domain (AD) followed by a C-terminal domain (CTD). (*b*) *In vitro* reaction of Uba5 57–363 with Ufm1 and Ufc1.The final concentrations of Uba5 57–363, Ufc1 and Ufm1 are 20, 40 and 100 µ*M*, respectively. Reactions were performed at 303 K for different times in 200 µl standard buffer consisting of 50 m*M* Tris–HCl pH 7.5, 150 m*M* NaCl, 5 m*M* $MgCl_2$, 1 m*M* ATP. 10 µl of the reaction products were then resolved by nonreducing 15% SDS–PAGE. The reaction times are labelled above the gel. The arrows indicate the positions of the recombinant proteins and the complexes formed. (*c*) *In vitro* reaction of Uba5 57–404 with Ufm1 and Ufc1; the same reaction system as in (*a*) was used. (*d*) GST pull-down analysis of the interaction between GST-tagged Uba5 CTD fragments and Ufc1. Proteins were incubated at 277 K for 1 h, pulled-down by a Glutathione Sepharose 4B column and analyzed using 15% nonreducing SDS–PAGE. Lanes L1, L2 and E show the loaded proteins of different Uba5 CTD fragments or GST, Ufc1 and the eluted proteins, respectively. Lane *M* in (*b*), (*c*) and (*d*) contains molecular-mass marker (labelled in kDa).

pGEX-6P-1 vector were transformed into *E. coli* BL21 (DE3) competent cells *via* a heat-shock procedure. The positive transformants were selected from agar plates containing 100 µg ml^{-1} ampicillin and were inoculated into 10 ml LB (Luria–Bertani) medium overnight at 310 K with agitation. The overnight cell culture was diluted into 1 l LB and grown under the same conditions to an OD_{600} of 0.6. Recombinant proteins were induced with 0.15 m*M* isopropyl *β*-D-1-thiogalactopyranoside (IPTG) at 291 K for 12 h.

The bacterial cells were harvested by centrifugation and resuspended in lysis buffer (50 m*M* Tris–HCl pH 8.0, 300 m*M* NaCl) supplemented with 10 m*M* $MgCl_2$, 200 U ml^{-1} DNaseI and 1 m*M* phenylmethanesulfonyl fluoride (PMSF), and then disrupted by sonication. The cell lysate was centrifuged at 8000*g* at 277 K for 45 min. For Uba5 57–363, Uba5 57–404, Ufc1 and Uba5 381–404~Ufc1, the cell lysate was first loaded onto an Ni–NTA column (Qiagen) and then eluted with elution buffer (50 m*M* Tris–HCl pH 8.0, 250 m*M* imidazole). For Uba5 330–404, 364–404 and 381–404, the cell lysate was loaded onto a Glutathione Sepharose 4B column (GE Healthcare) and then eluted with elution buffer (50 m*M* Tris-HCl pH 8.0, 10 m*M* GSH). The partially purified proteins were loaded onto a Source 15Q column (GE Healthcare) pre-equilibrated with 50 m*M* Tris–HCl pH 8.0 and then eluted using a linear gradient of 0–1 *M* NaCl. The fusion protein used for crystallization and Ufc1 used for the pull-down assay were treated with 3C protease (derived from rhinovirus) to remove the 6×His tag. Gly-Pro-His residues were left on the N-terminus of the fusion protein from the vector cloning sites. GST proteins used as control in pull-down assays were expressed by empty pGEX-6P-1 vector and subsequently treated with 3C protease, with Leu-Glu-Val-Leu-Phe-Gln residues left on the C-terminus from the vector cloning sites. Fractions were then condensed and loaded onto a Superdex 75 (GE Healthcare) column equilibrated with 10 m*M* Tris–HCl pH 8.0, 150 m*M* NaCl. Purified protein was analyzed by 12% SDS–PAGE and the protein concentration was determined by ultraviolet absorption at 280 nm (for recombinant Uba5 381–404~Ufc1, 1 A_{280} = 0.55 mg ml^{-1}). The purified fusion proteins concentrated to 15 mg ml^{-1} were aliquoted, frozen in liquid nitrogen and stored at 193 K for further experiments and crystallization.

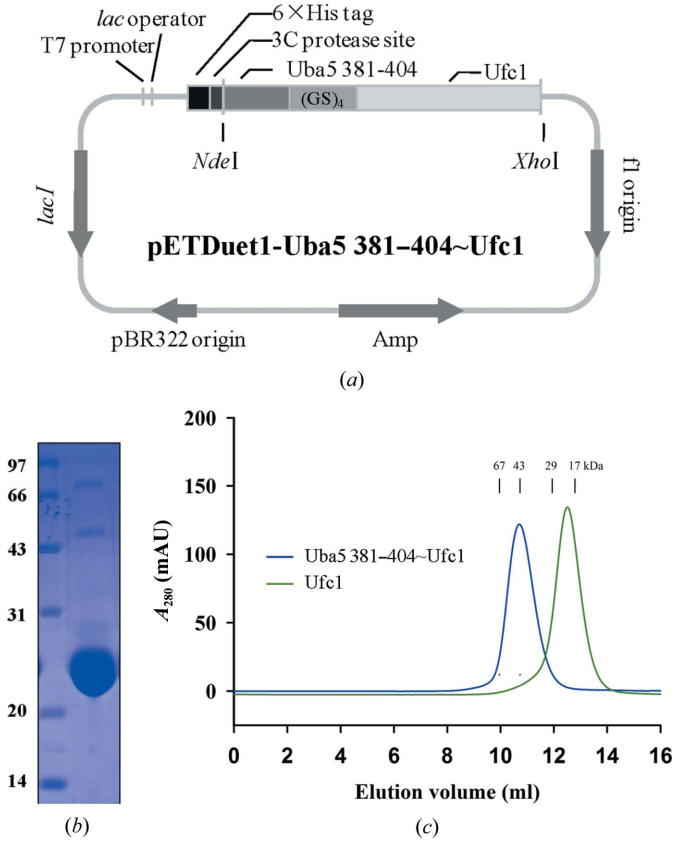

Figure 2
Cloning, expression and analysis of Uba5 381–404~Ufc1 fusion protein. (*a*) Expression vectors of the fusion protein. DNA fragments for the fusion protein were amplified and inserted into the pETDuet-1 vector with an N-terminal 6×His tag for recombinant expression. $(GS)_4$ indicates the four Gly-Ser repeat linker region. (*b*) Purification of the recombinant protein. The purified proteins were resolved *via* 15% SDS–PAGE, stained with Coomassie Brilliant Blue R-250 and then de-stained with an ethanol:acetic acid:water (2:1:7) mixture. The left lane contains the protein marker (labelled in kDa) and the right lane contains 1.5 µl of the purified recombinant fusion protein. (*c*) Oligomerization status of the fusion protein. The protein was analyzed using a Superdex 75 column. The standard markers indicated are 67, 43, 29 and 17 kDa.

Table 1
Data-collection and processing statistics for Uba5 381–404~Ufc1 fusion protein.

Values in parentheses are for the outer shell.

X-ray generator	Rigaku MicroMax-007
Wavelength (Å)	1.5419
Temperature (K)	100
Space group	$P6_2$ or $P6_4$
a, *b*, *c* (Å)	82.49, 82.49, 62.47
α, *β*, *γ* (°)	90.00, 90.00, 120.00
Mosaicity (°)	0.33
Resolution range (Å)	19.81–3.00 (3.21–3.00)
Total No. of reflections	109990
No. of unique reflections	4926
Completeness (%)	99.7 (100.0)
Multiplicity	22.3 (22.4)
$\langle I/\sigma(I)\rangle$	28.4 (2.0)
$CC_{1/2}$	1.000 (0.865)
$R_{r.i.m.}$	0.106 (1.879)
$R_{p.i.m.}$	0.022 (0.397)
R_{merge}† (%)	10.4 (183.6)

† $R_{merge} = \sum_{hkl}\sum_i |I_i(hkl) - \langle I(hkl)\rangle| / \sum_{hkl}\sum_i I_i(hkl)$.

2.3. *In vitro* reaction assay

Activation and transfer of Ufm1 to Ufc1 by Uba5 were analyzed by incubating the indicated concentrations of Uba5, Ufc1 and Ufm1 in a 200 µl reaction system. The reaction was performed at 303 K for different durations, then stopped using SDS–PAGE sample buffer (80 m*M* Tris–HCl pH 6.8, 2% SDS, 10% glycerol) and resolved by 15% nonreducing SDS–PAGE.

2.4. GST pull-down assay

Purified Ufc1 and GST-tagged Uba5 C-terminal fragments were mixed in a buffer consisting of 10 m*M* Tris–HCl pH 8.0, 150 m*M* NaCl and incubated for 1 h at 277 K. The mixtures were then loaded onto a Glutathione Sepharose 4B column and washed three times with incubating buffer. Subsequently, the bound proteins were eluted with elution buffer (50 m*M* Tris–HCl pH 8.0, 10 m*M* GSH) and analyzed by 15% nonreducing SDS–PAGE.

2.5. Crystallization

Crystallization of the Uba5 381–404~Ufc1 fusion protein was performed manually at 293 K *via* the hanging-drop method with different screening kits, including Crystal Screen, Index, PEG/Ion and SaltRx from Hampton Research and ProComplex Suite from Qiagen. 24-Well plates for crystallization (Beijing SeaskyBio Technology) were used with 1 ml reservoir buffer. Small irregular crystals

appeared in drops comprising 1.5 µl fusion-protein solution and 1.5 µl reservoir solution consisting of 100 m*M* HEPES–NaOH pH 7.0, 12–15%(*w*/*v*) PEG 4000, 0.1–0.3 *M* KCl after 2 d of growth. To improve X-ray diffraction quality, the crystals were subsequently optimized by microseeding. Droplets consisting of fusion-protein and reservoir solutions mixed in a 1:1 ratio were pre-equilibrated for 30 min against 1 ml reservoir solution. Several crystals that appeared in 100 m*M* HEPES–NaOH pH 7.0, 13%(*w*/*v*) PEG 4000, 0.16 *M* KCl were scooped up using a 0.1 mm loop (Hampton Research) and then transferred into a tube containing 45 µl seed-stock solution consisting of 100 m*M* HEPES–NaOH pH 7.0, 14%(*w*/*v*) PEG 4000, 0.2 *M* KCl. The crystals were broken up using a Seed Bead kit (Hampton Research) when vortex-mixed using 10 × 5 s bursts. The seed stock was diluted with the seed-stock solution to 1:10, 1:100 and 1:1000 ratios. Subsequently, 0.2 µl of seeds at the different dilutions were added to the pre-equilibrated 3.0 µl drops. The seed stocks were freshly prepared for each round of microseeding.

2.6. Data collection and processing

Fresh single crystals were harvested by transferring them with a cryoloop into cryoprotectant solution consisting of the reservoir solution supplemented with 25%(*v*/*v*) ethylene glycol and were then flash-cooled in liquid nitrogen. The diffraction data were collected in-house using a Rigaku MicroMax-007 X-ray generator equipped with a Saturn 944 CCD detector. Data sets were collected at 100 K with an exposure time of 60 s. The best crystal diffracted to 3.0 Å resolution using a crystal-to-detector distance of 75 mm with 1° oscillation per image. The complete data set was integrated using *XDS* (Kabsch, 2010) and scaled with *AIMLESS* (Evans, 2006).

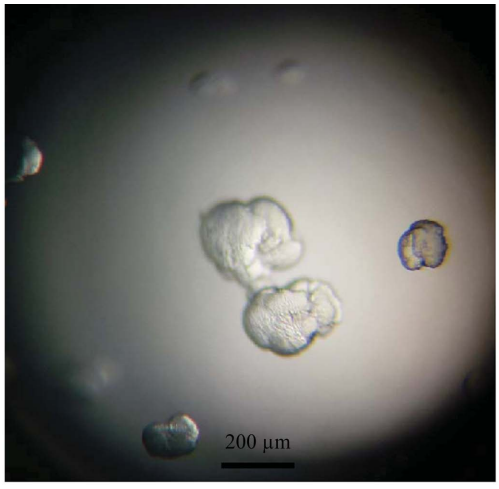

(*a*)

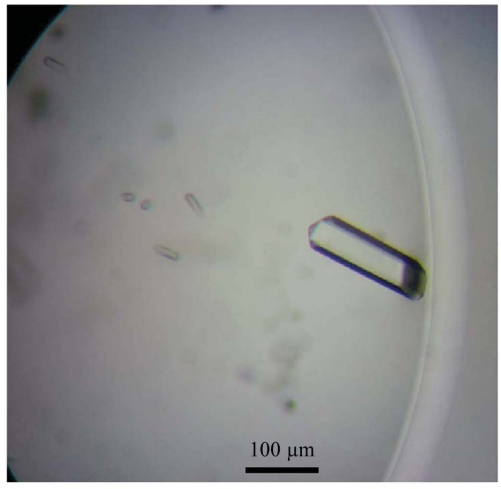

(*b*)

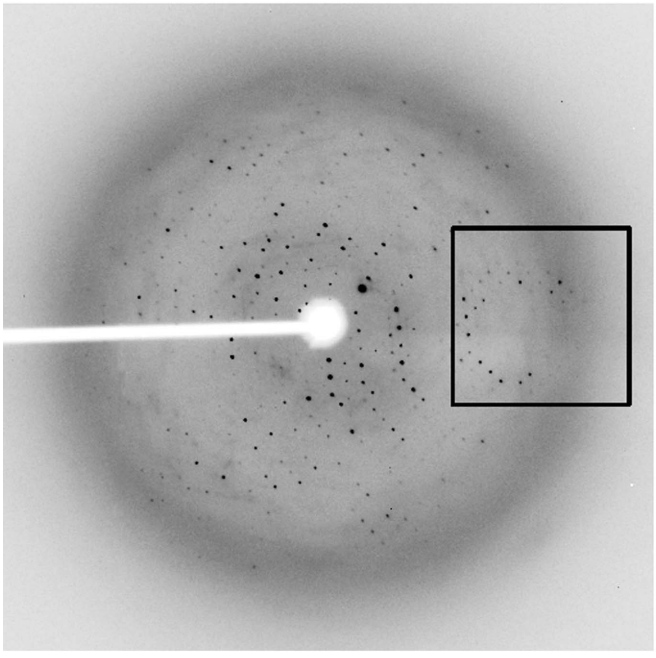

(*c*)

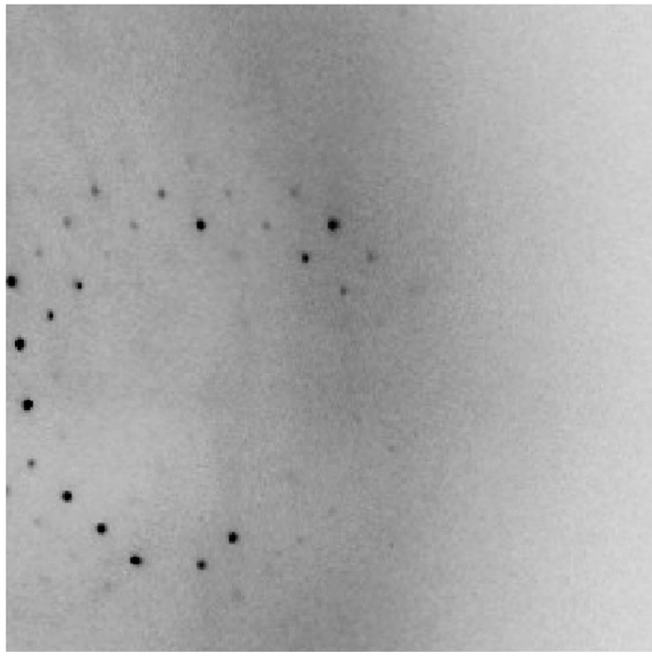

(*d*)

Figure 3
Preliminary X-ray crystallographic analysis of Uba5 381–404~Ufc1 fusion protein. (*a*) Crystals of the fusion protein. Crystals were obtained after 3 d at 293 K in crystallization buffer consisting of 100 m*M* HEPES–NaOH pH 7.0, 12–15%(*w*/*v*) PEG 4000, 0.1–0.3 *M* KCl. (*b*) Optimized crystals by microseeding in 100 m*M* HEPES–NaOH pH 7.0, 12%(*w*/*v*) PEG 4000, 0.15 *M* KCl, and 7 d of growth. (*c*) Diffraction pattern of the crystal. (*d*) Partial enlargement of the region in (*c*) surrounded by the rectangle.

3. Results and discussion

All canonical E1s possess a C-terminal ubiquitin-fold domain for recognition and recruitment of downstream E2s. In contrast, non-canonical E1s vary significantly in domain architecture, *e.g.* Atg7 recognizes Atg3 *via* an N-terminal domain consisting of a unique fold, which is located before the adenylation domain (Hong *et al.*, 2011; Noda *et al.*, 2011; Taherbhoy *et al.*, 2011). Our previous studies showed that Uba5 57–363 is the minimal fragment necessary for high-efficiency activation of Ufm1 (Xie, 2014). However, the molecular mechanism of Ufc1 recognition by Uba5 and the formation of the Ufc1–Ufm1 complex remain unknown.

To elucidate the functions of Uba5 364–404 in Ufm1 transthiolation, we conducted *in vitro* reactions using two truncations: Uba5 57–363 and 57–404. The yields of Uba5 57–363, 57–404 and Ufc1 were about 60, 48 and 42 mg per litre of culture, respectively. Uba5 57–363 failed to induce formation of the Ufc1–Ufm1 complex after 3 h of incubation in the system (Fig. 1*b*), while Uba5 57–404 leads to a co-migrating band of the Ufc1–Ufm1 complex after 20 min of reaction (Fig. 1*c*). Both truncations retain the ability to bind efficiently to Ufm1 in the reaction system. These results suggest that Uba5 residues 364–404, which are at the C-terminus, have no influence on the activation of Ufm1. However, they are necessary for the transfer of the activated Ufm1 to Ufc1. Subsequently, GST pull-down assays were conducted with untagged Ufc1 and three different GST-tagged Uba5 C-terminal region fragments (Fig. 1*d*). The yield of GST-tagged Uba5 330–404, 364–404, 381–404 and GST was about 45, 39, 42 and 56 mg per litre of culture, respectively. GST-tagged Uba5 330–404, 364–404 and 381–404 can strongly bind Ufc1, whereas GST alone cannot. This finding indicates that Uba5 381–404 is the minimal region for Ufc1 binding, which lies at the extreme C-terminal region of Uba5. Secondary-structural prediction reveals that this region probably forms an intact α-helix (Xie, 2014). Sequence analysis shows that this fragment is enriched in hydrophobic residues, which implies that the Ufc1 binding may be facilitated by hydrophobic interactions.

To further uncover the molecular mechanism of Uba5–Ufc1 recognition, the Uba5 381–404~Ufc1 fusion protein was expressed and purified, with a yield of about 50 mg per litre of culture, and its oligomerization status in solution was analyzed by gel-filtration chromatography (Fig. 2). The theoretical molecular mass of Uba5 381–404 was 2.66 kDa and that of Ufc1 was 19.4 kDa . The fusion of Uba5 381–404 and Ufc1 with a four Gly-Ser repeat linker region was therefore 22.6 kDa (Figs. 2*a* and 2*b*). Ufc1 eluted as monomers, whereas the fusion protein eluted as a homodimer in the gel-filtration assay (Fig. 2*c*). Given that the Uba5 C-terminal domain can interact with Ufc1, the formation of the homodimer may result from the intermolecular interactions between two fusion-protein molecules. Crystallographic studies on the Uba5 381–404~Ufc1 fusion protein were then performed (Fig. 3). The initial crystals had an irregular shape and very weak diffraction (Fig. 3*a*). Through microseeding, single rod-like crystals were visible after 2 d, and these crystals developed to their maximum dimensions, typically 100 × 40 × 40 µm, after 7 d. High-quality crystals suitable for data collection were obtained after microseeding in 100 m*M* HEPES–NaOH pH 7.0, 12%(*w*/*v*) PEG 4000, 0.15 *M* KCl for 7 d of growth (Fig. 3*b*).

X-ray diffraction data were collected to 3.0 Å resolution (Figs. 3*c* and 3*d*). The space group was determined to be $P6_2$ or $P6_4$. The unit-cell parameters were $a = b = 82.49$, $c = 62.47$ Å, $\alpha = \beta = 90$, $\gamma = 120^\circ$. With one fusion-protein molecule (22.6 kDa) in the crystallographic asymmetric unit, the calculated Matthews coefficient (V_M; Matthews, 1968) is 2.55 Å^3 Da^{-1} and the solvent content is 51.84%. The data statistics are presented in Table 1. Phase determination was attempted by molecular replacement using *Phaser* (McCoy *et al.*, 2007) with the structure of Ufc1 (PDB entry 2z6p; Mizushima *et al.*, 2007) as the search model. However, it failed even after several attempts. This may be due to conformational changes of Ufc1 induced by the Uba5 C-terminal region. Additional attempts at phase determination are in progress using multi-wavelength anomalous diffraction (MAD) and heavy-atom soaking.

We thank Dr Masaaki Komatsu for generously providing the cDNA plasmid of human Uba5 and Ufc1. This work was supported by 31070643 and 31130062 (Natural Science Foundation of China), 2011CB910803 and 2013CB530603 (China National Key Basic Research Program).

References

Bacik, J. P., Walker, J. R., Ali, M., Schimmer, A. D. & Dhe-Paganon, S. (2010). *J. Biol. Chem.* **285**, 20273–20280.
Dou, T., Gu, S., Liu, J., Chen, F., Zeng, L., Guo, L., Xie, Y. & Mao, Y. (2005). *Mol. Biol. Rep.* **32**, 265–271.
Evans, P. (2006). *Acta Cryst.* D**62**, 72–82.
Gannavaram, S., Sharma, P., Duncan, R. C., Salotra, P. & Nakhasi, H. L. (2011). *PLoS One*, **6**, e16156.
Goldberg, A. L. (2007). *Biochem. Soc. Trans.* **35**, 12–17.
Hertel, P., Daniel, J., Stegehake, D., Vaupel, H., Kailayangiri, S., Gruel, C., Woltersdorf, C. & Liebau, E. (2013). *J. Biol. Chem.* **288**, 10661–10671.
Hong, S. B., Kim, B.-W., Lee, K.-E., Kim, S. W., Jeon, H., Kim, J. & Song, H. K. (2011). *Nature Struct. Mol. Biol.* **18**, 1323–1330.
Kabsch, W. (2010). *Acta Cryst.* D**66**, 125–132.
Komatsu, M., Chiba, T., Tatsumi, K., Iemura, S., Tanida, I., Okazaki, N., Ueno, T., Kominami, E., Natsume, T. & Tanaka, K. (2004). *EMBO J.* **23**, 1977–1986.
Liu, G., Forouhar, F., Eletsky, A., Atreya, H. S., Aramini, J. M., Xiao, R., Huang, Y. J., Abashidze, M., Seetharaman, J., Liu, J., Rost, B., Acton, T., Montelione, G. T., Hunt, J. F. & Szyperski, T. (2009). *J. Struct. Funct. Genomics*, **10**, 127–136.
Matthews, B. W. (1968). *J. Mol. Biol.* **33**, 491–497.
McCoy, A. J., Grosse-Kunstleve, R. W., Adams, P. D., Winn, M. D., Storoni, L. C. & Read, R. J. (2007). *J. Appl. Cryst.* **40**, 658–674.
Mizushima, T., Tatsumi, K., Ozaki, Y., Kawakami, T., Suzuki, A., Ogasahara, K., Komatsu, M., Kominami, E., Tanaka, K. & Yamane, T. (2007). *Biochem. Biophys. Res. Commun.* **362**, 1079–1084.
Noda, N. N., Satoo, K., Fujioka, Y., Kumeta, H., Ogura, K., Nakatogawa, H., Ohsumi, Y. & Inagaki, F. (2011). *Mol. Cell*, **44**, 462–475.
Schulman, B. A. & Harper, J. W. (2009). *Nature Rev. Mol. Cell Biol.* **10**, 319–331.
Taherbhoy, A. M., Tait, S. W., Kaiser, S. E., Williams, A. H., Deng, A., Nourse, A., Hammel, M., Kurinov, I., Rock, C. O., Green, D. R. & Schulman, B. A. (2011). *Mol. Cell*, **44**, 451–461.
Tatsumi, K., Sou, Y.-S., Tada, N., Nakamura, E., Iemura, S., Natsume, T., Kang, S. H., Chung, C. H., Kasahara, M., Kominami, E., Yamamoto, M., Tanaka, K. & Komatsu, M. (2010). *J. Biol. Chem.* **285**, 5417–5427.
Tatsumi, K., Yamamoto-Mukai, H., Shimizu, R., Waguri, S., Sou, Y.-S., Sakamoto, A., Taya, C., Shitara, H., Hara, T., Chung, C. H., Tanaka, K., Yamamoto, M. & Komatsu, M. (2011). *Nature Commun.* **2**, 181.
Xie, S. (2014). *Acta Cryst.* F**70**, 765–768.
Zhang, Y., Zhang, M., Wu, J., Lei, G. & Li, H. (2012). *PLoS One*, **7**, e48587.
Zheng, M., Gu, X., Zheng, D., Yang, Z., Li, F., Zhao, J., Xie, Y., Ji, C. & Mao, Y. (2008). *J. Cell. Biochem.* **104**, 2324–2334.